NOISE ANALYSIS PREDICTS AT LEAST FOUR STATES FOR CHANNELS CLOSED BY GLUTAMATE

MARTIN WILSON, MARC TESSIER-LAVIGNE, AND DAVID ATTWELL
Department of Zoology, University of California, Davis, California 95616 and Department of Physiology, University College, London, England

ABSTRACT For ion channels that are opened by neurotransmitters, analysis of current noise has given valuable information on the kinetics of synaptic channel gating. In depolarizing bipolar cells of the vertebrate retina, we have recently characterized a synaptic current for which the neurotransmitter glutamate closes channels, and for which the channel open probability is low even in the absence of glutamate. We present here predictions for the current noise spectrum expected for various models of glutamate's action on the ion channels. Comparison of these theoretical predictions with experimental data allows us to rule out several simple kinetic schemes for the action of glutamate, and to conclude that the channels closed by glutamate must be able to exist in at least four different states.

INTRODUCTION

It was suggested by Kaneko (1971), and has since been supported by further evidence (Toyoda, 1973; Saito et al., 1978; Ashmore and Falk, 1980; Shiells et al., 1981; Nawy and Copenhagen, 1987), that the neurotransmitter released by photoreceptors in the vertebrate retina acts in an unusual way, in that it closes ion channels on one class of postsynaptic cells, the depolarizing bipolar cells. In a recent study of bipolar cells isolated from enzymatically dissociated axolotl retinae, we have found a fraction of cells, presumably the depolarizing bipolar cells, for which glutamate, the probable photoreceptor transmitter (Slaughter and Miller, 1985), decreases a membrane conductance (Attwell et al., 1987).

In order to investigate the molecular mechanism by which glutamate interacts with these channels we have applied the technique of fluctuation analysis to the drug-suppressed current. Although this approach has been widely applied to study channels opened by neurotransmitters, to our knowledge this is its first use for channels that are closed by neurotransmitter. An important constraint on the interpretation of our current fluctuation data arises from our finding that, even in the absence of glutamate, only a small fraction of the glutamate-gated channels are open. In this paper we use this constraint to define the types of kinetic scheme by which glutamate may interact with the channel. Consideration of these kinetic schemes leads to the prediction that the change of current fluctuations induced by glutamate will have a power spectrum with an unusual form. Although it is not yet possible to characterize completely the mechanism by which glutamate interacts with the channel, comparison of these theoretical predictions with our experimental data allows us to exclude all models in which the channel can exist in only two or three kinetically distinct states: the channel must be able to exist in at least four states.

Address correspondence to Dr. Marc Tessier-Lavigne, Howard Hughes Medical Institute, Columbia University, 722 West 168th St., New York, NY 10032.

EXPERIMENTAL RESULTS

In this section we present the experimental data used for comparison with the theoretical models analyzed below.

As discussed in detail elsewhere (Attwell et al., 1987), isolated bipolar cells that showed a conductance decrease in response to glutamate constituted 16% of all bipolar cells examined, with the other cells showing either an increase in conductance in response to glutamate (17%) or no response at all (67%).

The response of a typical conductance-decrease cell is shown in Fig. 1 *A*. This cell, when voltage-clamped at −54 mV, gave an outward current in response to glutamate. At more positive potentials the glutamate-induced current was inward: Fig. 1 *D* shows the current-voltage relation of the peak glutamate-evoked current. Since glutamate evokes a current that is outward below, and inward above its reversal potential, glutamate must be closing channels in the cell of Fig. 1. In addition to changing the mean membrane current, glutamate also decreased the noise in the current (Fig. 1, *B* and *C*). The decrease in current noise variance was proportional to the mean glutamate-induced current (Fig. 2 *A*). As shown in the Theory section below, this implies that the probability of the glutamate-gated channels being open is low, even in the absence of glutamate.

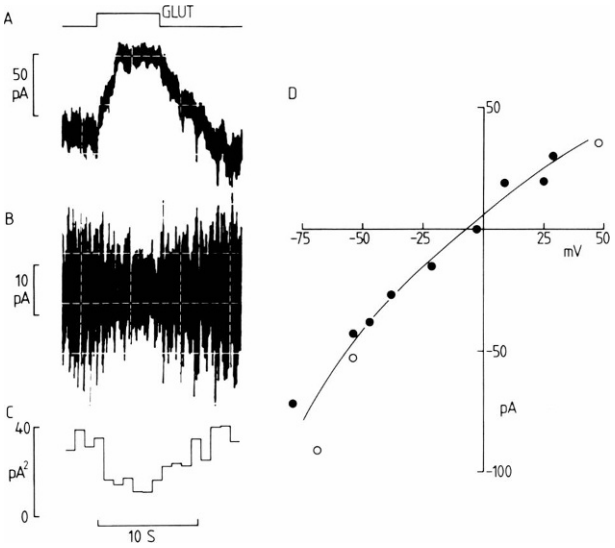

FIGURE 1 Glutamate closes ion channels in one class of retinal bipolar cell. (*A*) Current recorded in an isolated bipolar cell voltage-clamped at −54 mV, during superfusion of glutamate (1 mM), in Ringer's solution consisting of (millimolar): NaCl 88; KCl 1.5; $CaCl_2$ 3; $MgCl_2$ 0.5; $NaHCO_3$ 0.5; NaH_2PO_4 1; sodium pyruvate 1; glucose 15; Hepes 20; pH adjusted to 7.25 with NaOH. Patch pipette contained (millimolar): KCl 16.5; K-acetate 70; EGTA 5; $CaCl_2$ 0.5; NaCl 6; pH adjusted to 7.0 with KOH. Glutamate evokes an outward current and a decrease in current noise, which is seen more clearly in the high-pass (0.5 Hz, 8 pole) filtered trace (*B*) and the plot of variance (1–500 Hz) against time (*C*). (*D*) Voltage-dependence of the glutamate-suppressed current in the cell of parts *A–C* (○) and for a different cell in which a more complete I-V relation was obtained (●). The reversal potential of the glutamate-evoked current is ~0 mV. At negative potentials glutamate suppresses an inward current (plotted below the voltage axis) and at positive potentials it suppresses an outward current.

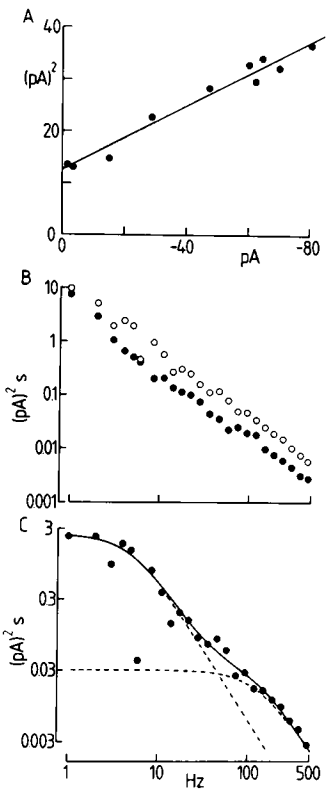

FIGURE 2 Current noise associated with the closing of channels by glutamate. (*A*) Variance (1–500 Hz) of the membrane current (ordinate) during the response in Fig. 1 *A*, as a function of inward current (abscissa: zero current position set arbitrarily). High variance occurs when a large inward current is flowing in the absence of glutamate. Variance is proportional to the current flowing through the glutamate-gated channels, indicating (Eq. 2) that the probability of channel opening is low. Slope of the best fit line is 0.3 pA. (*B*) Power spectrum (ordinate) of the current noise as a function of frequency (abscissa: scale as in *C*) before glutamate is applied (*open circles*) and in the presence of glutamate (*filled circles*). (*C*) Difference of the spectra of *B*: spectrum in the absence of glutamate minus spectrum in the presence of glutamate. Continuous curve is the sum of the two Lorentzians shown as dashed lines with parameters (see Eq. 1): $G(0)$ = 2.45 pA² s, f_c = 5 Hz for the low frequency Lorentzian; and $G(0)$ = 0.03 pA² s, f_c = 135 Hz for the high frequency Lorentzian.

In order to study the frequency dependence of the current fluctuations, we have calculated their power spectrum. Fig. 2 *B* shows the spectrum of the current fluctuations in the absence and presence of glutamate. The difference between these two curves is shown in Fig. 2 *C*, which represents the spectrum of the current fluctuations suppressed by glutamate. Fig. 2 *C* also shows that in the frequency range 1–500 Hz, the spectrum can be fitted by the sum of two Lorentzian curves of the form:

$$G(0)/[1 + (f/f_c)^2], \qquad (1)$$

where f is the frequency, $G(0)$ is the zero frequency asymptote of the function, and f_c is the half power frequency. The two Lorentzians used to fit the spectrum in Fig. 2 *C* are shown as dashed lines, and their sum is shown as a full line. The power spectra we measured in seven cells all required the sum of two Lorentzian curves to fit them. On average, the half power frequencies of the two Lorentzians were f_c = 8.3 ± 2.0 Hz for the low frequency component, and f_c = 185 ± 93 Hz for the high frequency component. The implications of the shape of the spectra are discussed in the next section.

THEORY

In this section, we consider several kinetic schemes for how glutamate closes channels on postsynaptic depolarizing bipolar cells. We assume, for simplicity, that glutamate acts directly on the channels, although the same analysis would apply if glutamate acted by raising the concentration of an intracellular messenger that acted on the channels (e.g., inositol trisphosphate: Sugiyama et al., 1987). All the channels are assumed to have the same kinetic properties. We start with the simplest two- and three-state models and show that they cannot explain certain features of the glutamate-evoked conductance changes described in the Results. We then show that this is also true of more complex three-state models, although some four-state models can explain our observations.

(*A*) Inadequacy of the Simplest Models to Explain the Actions of Glutamate

As described above, in depolarizing bipolar cells the conductance decrease produced by glutamate was associated with a decrease in current noise (see Figs. 1 *B* and 2 *A*). This immediately rules out the two simplest models that can be postulated to explain how glutamate closes chan-

nels:

$$T + \underset{\text{open}}{R^*} \rightleftarrows \underset{\text{blocked}}{TR}$$

Model I

$$T + \underset{\text{open}}{R^*} \rightleftarrows \underset{\text{open}}{TR^*} \rightleftarrows \underset{\text{closed}}{TR}.$$

Model II

Model I is a simple channel blocking model: the transmitter (T) is assumed to block channels that are open in its absence (R*). In Model II, transmitter binds to a receptor on an open channel, forming an open transmitter-receptor complex (TR*) which can then close. This model is, for transmitters that close channels, the equivalent of the simple sequential binding and opening model (Magleby and Stevens, 1972; Katz and Miledi, 1972), that has been invoked to explain how other transmitters (e.g., acetylcholine) open channels.

Both of these models predict that glutamate should, at least at low doses, increase the membrane current noise, for the following reason. In general, the current noise generated by a number, N, of identical channels is (Colquhoun and Hawkes, 1977):

$$\text{current variance} = N \cdot i^2 p(1 - p), \qquad (2)$$

where i is the current flowing through a channel when it is open, and p is the channel open probability. In both models above, in the absence of transmitter the channels are open all the time ($p = 1$), and from Eq. 2 the current variance is zero. Adding transmitter will cause a reduction in p in both models, which, from Eq. 2, will lead to an increase in current variance. As p is further decreased, the current variance will continue increasing, reach a maximum when $p = 0.5$, then start decreasing. Since glutamate is found experimentally to cause a decrease in current variance, in its absence p must be <0.5, which rules out Models I and II. For low values of p, Eq. 2 predicts a linear relationship between noise variance and current, as seen in Fig. 2 *A*.

(*B*) Three-State Models Compatible With a Glutamate-evoked Noise Decrease

Although the finding that the channels' open probability is <0.5 in the absence of glutamate rules out the simple models shown above for the action of glutamate, the following three-state models are compatible with this finding:

$$\underset{\text{closed}}{R} \overset{\beta}{\underset{\alpha}{\rightleftarrows}} \underset{\text{open}}{R^*} \overset{T + k_1}{\underset{k_2}{\rightleftarrows}} \underset{\text{blocked}}{TR}$$

Model III

$$\underset{\text{open}}{R^*} \overset{\alpha}{\underset{\beta}{\rightleftarrows}} \underset{\text{closed}}{R} \overset{T + k_1}{\underset{k_2}{\rightleftarrows}} \underset{\text{closed}}{TR}.$$

Model IV

In both models, in the absence of transmitter (T) the channel can exist in two states, open (R*) or closed (R). In Model III, transmitter is postulated to block the open channel. In Model IV, transmitter is postulated to combine with the closed channel, allowing it to enter another closed state (TR). The fraction of channels that are open in the absence of transmitter is $\beta/(\alpha + \beta)$, where α and β are the channel closing and opening rates, respectively. Thus, if $\beta < \alpha$, the open probability is <0.5 in the absence of transmitter. These are the only three-state models that can explain the noise decrease that we find associated with the glutamate-evoked conductance decrease.

To test whether either of these models could also account for the kinetic properties of the glutamate-gated channels, we have calculated the power spectra predicted from Models III and IV using the equations of Colquhoun and Hawkes (1977). We now show that the difference spectra generated by these models are not even approximately similar to the experimentally measured difference spectrum showed in Fig. 2 *C*.

In both Model III and Model IV, in the absence of transmitter the channel can exist in only two states, one open and one closed. The power spectrum of the fluctuations in the current through the channels will therefore be a single Lorentzian with half power frequency $f_c = (\alpha + \beta)/2\pi$ (Colquhoun and Hawkes, 1977). When a nonsaturating amount of transmitter is added, the channel can exist in three states, so that the spectrum of the fluctuations in current through the channels (not the difference spectrum) is the sum of two Lorentzian curves (Colquhoun and Hawkes, 1977):

$$G(f) = G_1/[1 + (f/f_1)^2] + G_2/[1 + (f/f_2)^2], \qquad (3)$$

where $G(f)$ is the spectral density at frequency f, G_1, and G_2 are the zero-frequency asymptotes of the two Lorentzian curves, and f_1 and f_2 are their respective corner frequencies. Expressions for the dependence of G_1, G_2, f_1, and f_2 on the rate constants and transmitter concentration in Models III and IV are given below. The difference spectrum of the glutamate-suppressed current is obtained by subtracting the two Lorentzian spectrum of Eq. 3 from the single Lorentzian spectrum occurring in the absence of glutamate.

Expressions were derived for the parameters G_1, G_2, f_1, and f_2 from Eqs. 11, 14, 15, 46, and 89–94 of Colquhoun and Hawkes (1977). The results were as follows. For Model III:

$$G_1 = (Ni^2) \cdot [4\beta k_2/(L_1 L_2)] \cdot (1 - \beta/L_1) \cdot (1 - k_2/L_1)/(L_1 - L_2) \qquad (4)$$

$$G_2 = (Ni^2) \cdot [4\beta k_2/(L_1 L_2)] \cdot (1 - \beta/L_2) \cdot (1 - k_2/L_2)/(L_2 - L_1) \qquad (5)$$

$$f_1 = L_1/2\pi; \quad \text{and} \quad f_2 = L_2/2\pi, \qquad (6)$$

where L_1 and L_2 are solutions of:

$$L^2 - (\alpha + \beta + k_2 + k_1 \cdot [T]) \cdot L + (\alpha k_2 + \beta k_2 + \beta k_1 \cdot [T]) = 0. \quad (7)$$

For Model 4:

$$G_1 = (\mathrm{Ni}^2) \cdot (4\alpha\beta k_1 k_2 \cdot [T]/L_1^2) \cdot (1 - \alpha/L_2)/[(1 - k_2/L_2) \cdot (L_2 - L_1)] \quad (8)$$

$$G_2 = (\mathrm{Ni}^2) \cdot (4\alpha\beta k_1 k_2 \cdot [T]/L_2^2) \cdot (1 - \alpha/L_1)/[(1 - k_2/L_1) \cdot (L_1 - L_2)] \quad (9)$$

$$f_1 = L_1/2\pi; \quad \text{and} \quad f_2 = L_2/2\pi, \quad (10)$$

where L_1 and L_2 are solutions of:

$$L^2 - (\alpha + \beta + k_2 + k_1 \cdot [T]) \cdot L + (\alpha k_2 + \beta k_2 + k_1 \cdot [T]) = 0. \quad (11)$$

The range of behavior of the nondifference spectra (Eq. 3) predicted for Model III can be seen in Fig. 3, *B* and *D*, which were chosen to show two different sets of rate constants: $\beta = \alpha/2$, $k_2 = \alpha/20$, and $\beta = \alpha/4$, $k_2 = 5\alpha$, respectively. As shown in Fig. 3 *D*, increasing transmitter concentration can drive down the low frequency asymptote or alternatively (Fig. 3 *B*) drive it up for small amounts of transmitter and down again for higher concentrations. Increasing transmitter concentrations from zero can either move the high frequency asymptote to the right on a log-log plot (Fig. 3 *D*) or to the left (Fig. 3 *B*).

In Fig. 3, *C* and *E* we plot the difference spectra, obtained by subtracting the curves in Fig. 3, *B* and *D*, respectively from the single Lorentzian nondifference spectrum occurring in the absence of transmitter (shown for $[T] = 0$ in Fig. 3, *B* and *D*). The difference spectrum takes negative values (undefined in our log-log plots) wherever the low frequency asymptote of the nondifference spectrum in the presence of drug is above that in its absence, or where the high frequency asymptote with drug lies to the right of the asymptote without drug. This accounts for the precipitous drop in some difference spectra at low (Fig. 3 *C*) or high frequencies (Fig. 3 *E*). In fact, although not indicated here, sets of rate constants and transmitter concentrations can be found that produce negative densities in the difference spectrum at both high and low frequencies. Peaked difference spectra are easily generated by Model III but no choice of parameters can give rise to difference spectra resembling our experimental data (Fig. 2 *C*): at high frequencies the difference spectra in Fig. 3 decrease with a slope of -2, while our experimental spectra decrease with a smaller slope ($\sim$1.3) between 3 and 300 Hz, and require the sum of two Lorentzians to fit them in this range.

This same general conclusion holds for Model IV, whose spectra are illustrated in Fig. 4. The range of behavior for this model is more restricted than for Model III since

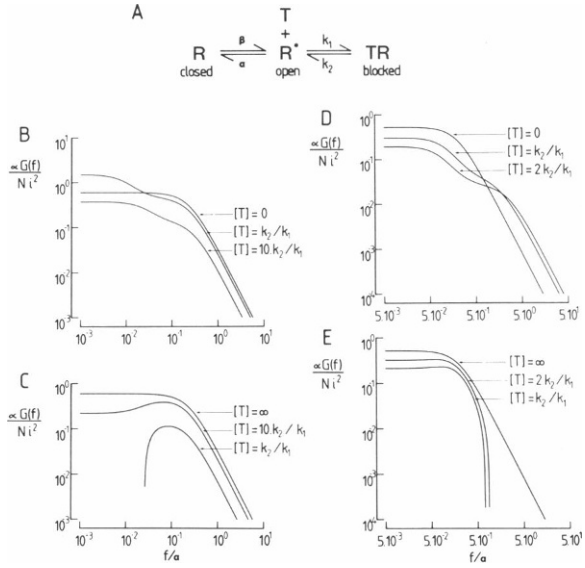

FIGURE 3 Noise spectra predicted for Model III (*A*), in which the transmitter (*T*) glutamate is postulated to block open channels. (*B*) Noise spectra (not difference spectra) of the current flowing through the glutamate-sensitive channels, as a function of frequency (plotted as the dimensionless variable f/α), for different concentrations, $[T]$, of the transmitter glutamate (shown by each curve). Noise power is plotted as the dimensionless variable $\alpha G/\mathrm{Ni}^2$. For all three curves, the rate constants in *A* were set so that $\beta = \alpha/2$ and $k_2 = \alpha/20$. In the absence of transmitter ($[T] = 0$) the channels flick between open and closed states and thus generate a single Lorentzian spectrum. For nonzero values of $[T]$, all three states of the kinetic scheme (*A*) are possible, and so the spectrum is the sum of two Lorentzians. (*C*) Difference spectra (as would be measured experimentally) obtained by subtracting the spectrum at a nonzero value of $[T]$ in *B* from the spectrum plotted in *B* for $[T] = 0$ (no transmitter present). The spectrum for $[T] = \infty$ is the same as that for $[T] = 0$ in *B*. (*D, E*) Nondifference and difference spectra, as in *B* and *C*, respectively, but with $\beta = \alpha/4$ and $k_2 = 5\alpha$.

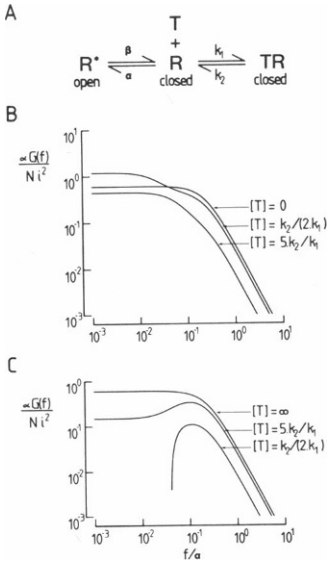

FIGURE 4 Noise spectra predicted for Model IV (*A*) in which the transmitter (*T*) glutamate is postulated to bind to a receptor on a closed channel, allowing it to enter another closed state. (*B*) Noise spectra (plotted on the ordinate in terms of the dimensionless variable $\alpha G/\mathrm{Ni}^2$) as a function of frequency (plotted as the dimensionless variable f/α), for the current through the glutamate-sensitive channels (not difference spectra). Concentration of glutamate is shown by each curve. For all the curves, the rate constants were set so that $\beta = \alpha/2$ and $k_2 = \alpha/10$. (*C*) Difference spectra (as would be recorded experimentally), obtained by subtracting the spectrum at a nonzero value of $[T]$ in *B* from the spectrum plotted in *B* for $[T] = 0$. The spectrum for $[T] = \infty$ is the same as that for $[T] = 0$ in *B*.

increasing transmitter concentration always moves the high frequency asymptote of the nondifference spectrum to the left. The low frequency asymptote, however, like that of the previous model, can go down with increasing transmitter concentrations or it can go up first and then down at high concentrations. Again, however, no spectra even approximately similar to our experimental difference spectra data can be generated.

Four-State Model for the Action of Glutamate

A simple modification of Model III can predict a glutamate-induced noise decrease which has a difference spectrum described by the sum of two Lorentzians. A four-state scheme such as:

$$\underset{\text{closed}}{R'} \rightleftarrows \underset{\text{closed}}{R} \rightleftarrows \underset{\text{open}}{R^*} \rightleftarrows \underset{\text{blocked}}{TR} \qquad (T + \cdot)$$

Model V

would generate a two Lorentzian spectrum for the current noise in the absence of transmitter, and in the presence of excess glutamate all the channels would be closed and contribute no noise. The difference spectrum would thus be the sum of two Lorentzians (at least for the case of a saturating dose of glutamate).

The same would be true of the following modification of Model IV:

$$\underset{\text{closed}}{R'} \rightleftarrows \underset{\text{open}}{R^*} \rightleftarrows \underset{\text{closed}}{R} \rightleftarrows \underset{\text{closed}}{TR}. \qquad (T + \cdot)$$

Model VI

In both Model V and Model VI, another closed state (R') has simply been added to the left of the first state in Models III and IV, respectively. Other, more complex modifications of Models III and IV can obviously also result in two Lorentzian spectra. To distinguish between the different models, and determine exactly how glutamate closes channels on putative depolarizing bipolar cells, will probably require examining the effect of glutamate on single channels using cell-attached or outside-out patch-clamp techniques. Nevertheless, the method of noise analysis used here has permitted a partial characterization of the mechanism by which glutamate closes channels, and the rejection of a number of simple models. The channel that is closed by glutamate must be able to exist in at least four different states.

DISCUSSION

Since reports of channels closed by neurotransmitters and other agents are less common than those opened by these agents, our understanding of the molecular mechanisms by which channels are closed is presently very slight. Comparison of experimental and predicted current fluctuations presented here leads to the conclusion that in retinal bipolar cells the kinetics of the channels closed by glutamate are complex, involving at least four states and resulting in a channel open probability that is small even in the absence of neurotransmitter. An analogous situation has been described for a K^+ channel in skeletal muscle (Spruce et al., 1985) where intracellular ATP closes a channel that can exist in at least two open states and three closed states. Like the channel we describe here, the skeletal muscle channel is not always open in the absence of ATP; in fact, its probability of being open is 0.5, and is reduced by a factor of ~3 in the presence of millimolar ATP.

Kaneko and Tachibana (1985) have described the closure of channels by glutamate in another kind of retinal cell: the horizontal cell of goldfish. Their experiments suggest that glutamate works by blocking channels, a possible mechanism by which glutamate may close channels in bipolar cells. Nevertheless it is clear that the channel they describe is not the same as that described here, since theirs has the characteristics of an anomalous rectifying K^+ channel while in bipolar cells this is not the case (Fig. 1 *D*).

Supported by the Medical Research Council, National Institutes of Health (EY 04112 to Martin Wilson), the Royal Society, the Wellcome Trust, North Atlantic Treaty Organization (Collaborative Research grant RG 85/0471), and the Central Research Fund of London University.

Received for publication 6 April 1987.

REFERENCES

Ashmore, J. F., and G. Falk. 1980. Responses of rod bipolar cells in the dark-adapted retina of the dogfish, *Scyliorhinus canicula*. *J. Physiol. (Lond.)*. 300:115–150.

Attwell, D., P. Mobbs, M. Tessier-Lavigne, and M. Wilson. 1987. Neurotransmitter-induced currents in retinal bipolar cells of the axolotl, *Ambystoma mexicanum*. *J. Physiol. (Lond.)*. 387:125–161.

Colquhoun, D., and A. G. Hawkes. 1977. Relaxation and fluctuations of membrane currents that flow through drug-operated channels. *Proc. R. Soc. Lond. B. Biol. Sci.* 199:231–262.

Kaneko, A. 1971. Physiological studies of single retinal cells and their morphological identification. *Vision Res.* 3 (Suppl.):17–26.

Kaneko, A., and M. Tachibana. 1985. Effects of L-glutamate on the anomalous rectifier channels in horizontal cells of *Carassius auratus* retina. *J. Physiol. (Lond.)*. 358:169–182.

Katz, B., and R. Miledi. 1972. The statistical nature of the acetylcholine potential and its molecular components. *J. Physiol. (Lond.)*. 224:665–699.

Magleby, K. L., and C. F. Stevens. 1972. A quantitative description of end-plate currents. *J. Physiol. (Lond.)*. 223:173–197.

Nawy, S., and D. R. Copenhagen. 1987. Multiple classes of glutamate receptor in depolarizing bipolar cells in retina. *Nature (Lond.)*. 325:56–58.

Saito, T., H. Kondo, and J. Toyoda. 1978. Rod and cone signals in the on-centre bipolar: their different ionic mechanisms. *Vision Res.* 18:591–595.

Shiells, R. A., G. Falk, and S. Naghshineh. 1981. Action of glutamate and aspartate analogues on rod horizontal and bipolar cells. *Nature (Lond.)*. 294:592–594.

Slaughter, M. M., and R. F. Miller. 1985. Characterization of an extended glutamate receptor of the on bipolar neuron in the vertebrate retina. *J. Neurosci.* 5:224–233.

Spruce, A. E., N. B. Standen, and P. R. Stanfield. 1985. Voltage-dependent ATP-sensitive potassium channels of skeletal muscle membrane. *Nature* (*Lond.*). 316:736–738.

Sugiyama, H., I. Ito, and C. Hirono. 1987. A new type of glutamate receptor linked to inositol phospholipid metabolism. *Nature* (*Lond.*). 325:531–533.

Toyoda, J. 1973. Membrane resistance changes underlying the bipolar response in carp retina. *Vision Res.* 13:283–294.